COMPLEX NONLINEARITIES FOR AUDIO SIGNAL PROCESSING

Jatin Chowdhury

Center for Computer Research in Music and Acoustics
Stanford University
Palo Alto, CA
jatin@ccrma.stanford.edu

ABSTRACT

In this writing, we present an ongoing study of new and interesting nonlinear structures for audio signal processing, intended to be used for audio effects and synthesis. We give a brief discussion of each structure, and present a series of open-source audio plugins that implement the structures.

1. INTRODUCTION

In digital audio signal processing it is common to find audio effects that use nonlinear elements to add harmonic content to the signal being processed, or to achieve a "distortion" type of effect. Typically, this is done either as part of an analog model, or using a static memoryless nonlinear element.

The goal of this research project is to develop structures for nonlinear audio signal processing that go beyond the traditionally used simple nonlinearities. While the structures developed here may be used for analog modelling and may be inspired by analog effects, they do not come about from direct physical modelling of an analog system, nor do they require knowledge of analog systems such as circuits to be understood and implemented.

1.1. Simple Nonlinearities

We refer to the desired nonlinear structures as "Complex Nonlinearities", as such we should take a moment to define what constitutes a "simple" nonlinearity, particularly since these will make up the building blocks of the complex nonlinearities that follow.

1.1.1. Saturators

The most commonly used nonlinearity in audio signal processing is the saturating nonlinearity, where the input "clips" to a constant value as the input gain increases. This class of nonlinearity includes functions such as the hard clipper, cubic soft clipper, and $tanh$ nonlinearities [1], which are described by the following functions:

$$f_{\text{hard clip}}(x) = \begin{cases} -1 & x < -1 \\ x & -1 \leq x \leq 1 \\ 1 & x > 1 \end{cases} \tag{1}$$

$$f_{\text{soft clip}}(x) = \begin{cases} -\frac{2}{3} & x < -1 \\ x - \frac{x^3}{3} & -1 \leq x \leq 1 \\ \frac{2}{3} & x > 1 \end{cases} \tag{2}$$

$$f_{\tanh}(x) = \tanh(x) \tag{3}$$

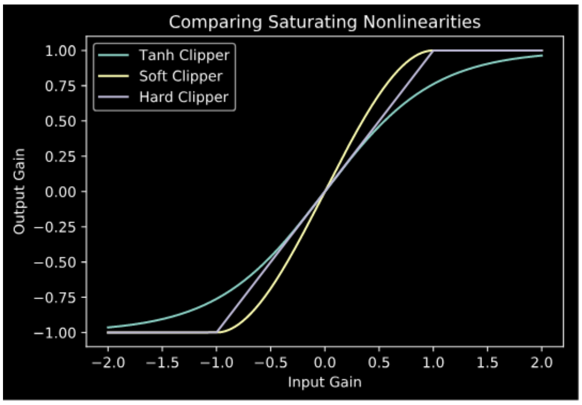

Figure 1: *Saturating Nonlinearities*

1.1.2. Rectifiers

Sometimes for audio effects such as compressors and limiters, it is useful to have a rectified signal (i.e. a signal that only contains non-negative values). The two most simple rectifying nonlinearities are the full-wave rectifier and the half-wave rectifier:

$$f_{\text{FWR}}(x) = |x| \tag{4}$$

$$f_{\text{HWR}}(x) = \begin{cases} 0 & x < 0 \\ x & x \geq 0 \end{cases} \tag{5}$$

The above rectifier equations have a downside in that they don't have continuous derivatives. As a substitute we present an alternate half-wave rectifier equation loosely modelled from a Shockley diode rectifier:

$$f_{\text{Diode}}(x) = \beta\left(e^{\alpha x} - 1\right) \tag{6}$$

where α and β are tunable parameters.

1.1.3. Dropout

Another nonlinearity used in audio effects is the "dropout" nonlinearity, notably used for modelling underbiased analog tape recording [2]. A dropout nonlinearity is characterized by the fact that small input values are snapped to zero. Here we present a simple cubic dropout function:

$$f_{\text{Dropout}}(x) = \begin{cases} x + B - \left(\frac{B}{a}\right)^3 & x < -B \\ \left(\frac{x}{a}\right)^3 & -B \leq x \leq B \\ x - B + \left(\frac{B}{a}\right)^3 & x > B \end{cases} \tag{7}$$

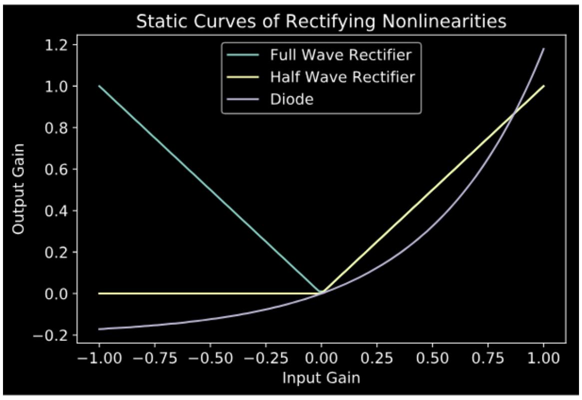

Figure 2: *Rectifying Nonlinearities. For the diode nonlinearity, we use* $\beta = 0.2$*,* $\alpha = 1.93$*.*

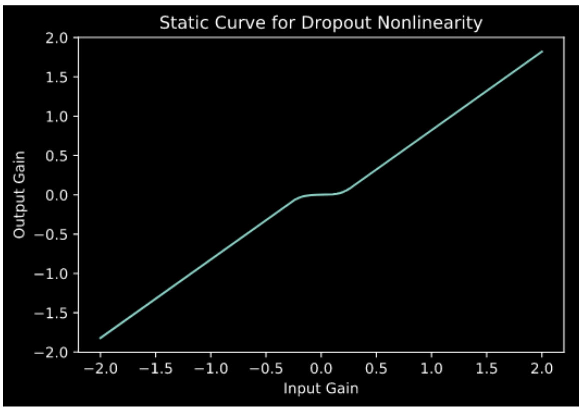

Figure 3: *Dropout nonlinearity with* $a = 0.6$*.*

where a is a tunable parameter, and $B = \sqrt{\frac{a^3}{3}}$.

2. DOUBLE SOFT CLIPPER

The Double Soft Clipper (see fig. 4) is a sort of combination between a saturating nonlinearity and dropout nonlinearity. The nonlinear function is given as:

$$f_{\text{DSC}}(x) = \begin{cases} 1 & u \geq 1 \\ (3/4) * (u - u^3/3) + 0.5 & 0 < u < 1 \\ (3/4) * (u - u^3/3) - 0.5 & -1 < u < 0 \\ -1 & u \leq -1 \end{cases} \tag{8}$$

where

$$u(x) = \begin{cases} x - 0.5 & x > 0 \\ x + 0.5 & x < 0 \end{cases} \tag{9}$$

The resulting static curve is essentially two cubic soft clipping functions stacked on top of each other (see fig. 5). One advantage of this nonlinear function is that it is highly parameterizable. Possible parameters include upper/lower clipping limit, linear slope, upper/lower skew, and dropout width (see fig. 6).

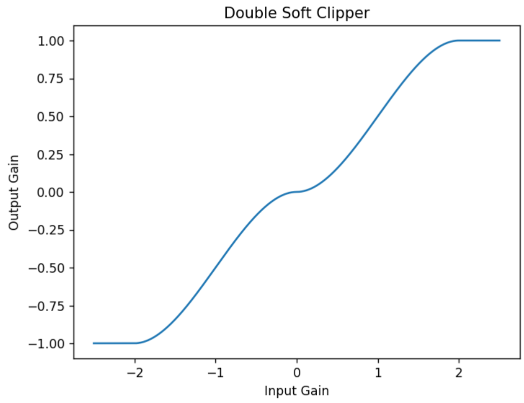

Figure 4: *Double soft clipper.*

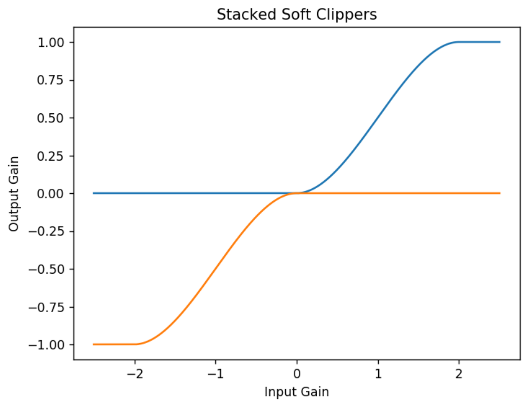

Figure 5: *Stacked soft clippers.*

3. HARMONIC EXCITER

A harmonic exciter is an audio effect often used by mixing engineers to add “brightness” to a track or a mix, for example the Aphex Aural Exciter [3]. Typically, digital exciter effects are implemented as circuit models of an original analog effect (e.g. [4]). The goal of this work is to create a generalized exciter model that can be implemented without knowledge of circuit theory, much in the way that [5] describes a generalized model of a dynamic range compressor.

Based loosely on the Aphex Aural Exciter, we propose the exciter architecture shown in fig. 7. For the generator component, we propose the processing architecture shown in fig. 8.

For the level detector component, we propose using a rectifying nonlinearity followed by a lowpass filter. Figure 9 shows the output of a level detector with the rectifying nonlinearities described in §1.1.2 and a first-order lowpass filter with a cutoff frequency of 10 Hz. For the nonlinearity component, any saturating nonlinearity of the type described in §1.1.1 will suffice. The output of the generator is very harmonically rich, with both even and odd harmonics, as seen in fig. 11.

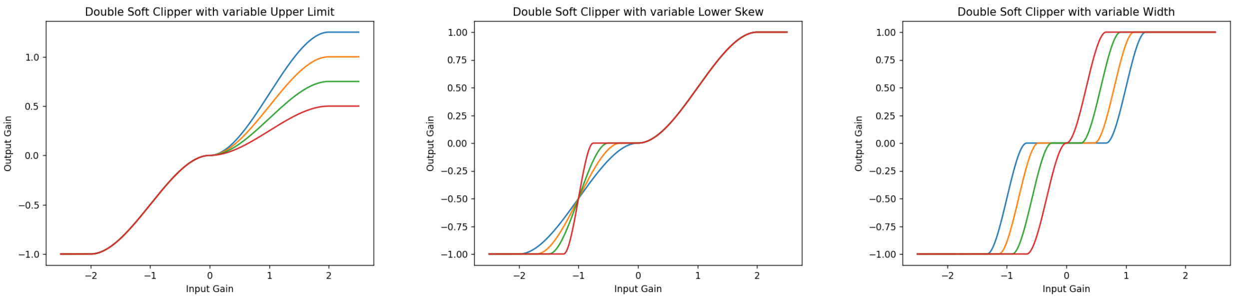

Figure 6: *Double soft clippers with variable upper clipping limit (left), variable lower skew (middle), and variable dropout width (right).*

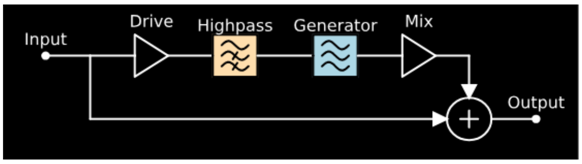

Figure 7: *Exciter architecture.*

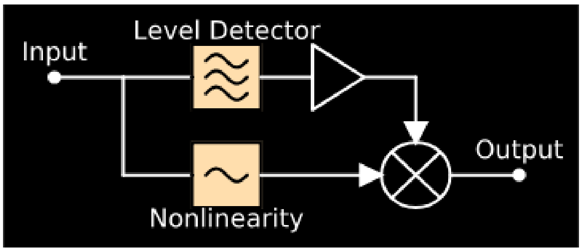

Figure 8: *Exciter generator architecture.*

4. HYSTERESIS

Hysteresis is an interesting complex nonlinear behavior that describes the magnetising of magnetic materials, as well as concepts in other fields including chemistry, structural engineering, even economics. [2] uses an adaptation of the Jiles-Atherton magnetic hysteresis model to recreate the sound of an analog tape machine. In this study, we attempt to generalize this hysteresis model to be used and implemented without understanding of electromagnetic physics, as well as adding useful parameters to the hysteresis nonlinearity.

The hysteresis model for input x is defined by the differential equation:

$$\dot{y} = \frac{\frac{(1-c)\delta_y(SL(Q)-y)}{(1-c)\delta_x k-\alpha(SL(Q)-y)}\dot{x} + c\frac{S}{a}\dot{x}L'(Q)}{1-c\alpha\frac{S}{a}L'(Q)} \tag{10}$$

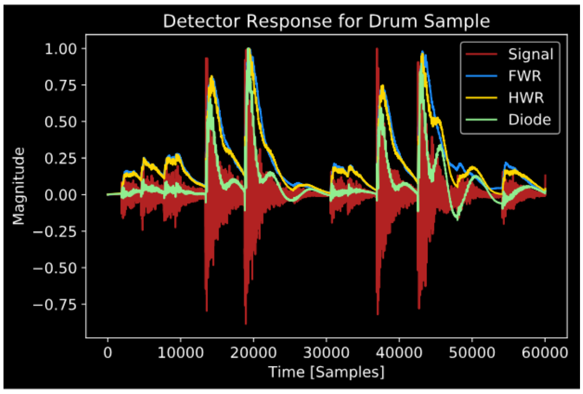

Figure 9: *Exciter level detector.*

where $\dot{y}$ denotes the time derivative of the output, and k and a are constant values. δ_x and δ_y are defined as

$$\delta_x = \begin{cases} 1 & \text{if } x \text{ is increasing} \\ -1 & \text{if } x \text{ is decreasing} \end{cases} \tag{11}$$

$$\delta_y = \begin{cases} 1 & \text{if } \delta_x \text{ and } L(Q)-y \text{ have the same sign} \\ 0 & \text{otherwise} \end{cases} \tag{12}$$

$L(x)$ denotes the Langevin function:

$$L(x) = \coth(x) - \frac{1}{x} \tag{13}$$

and Q is defined as

$$Q(x,y) = \frac{x+\alpha y}{a} \tag{14}$$

where α is a constant value, and x and y are the system input and output respectively.

The variables S, a, and c from eq. (10) can be used as parameters to control the hysteresis function saturation, drive, and width respectively. Figure 10 shows the effects of modulating these parameters.

5. NONLINEAR BIQUADS

Transposed Direct Form II (TDF-II) (see fig. 12) is a standard method for implementing biquad filters in signal processing. We

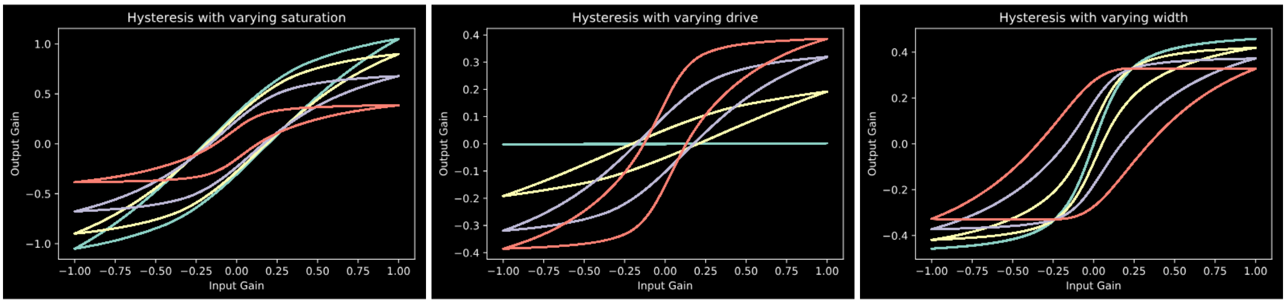

Figure 10: *Hysteresis curves with variable saturation (left), drive (middle), and width (right).*

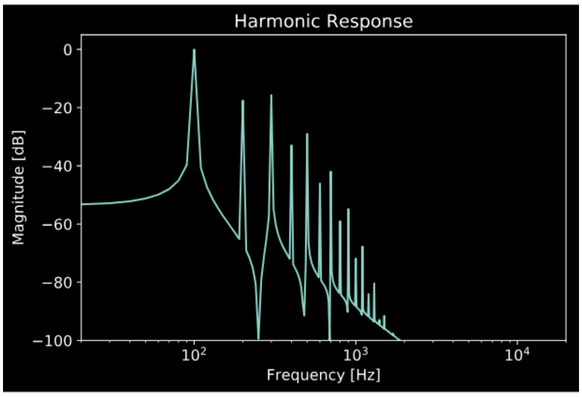

Figure 11: *Exciter generator harmonic response.*

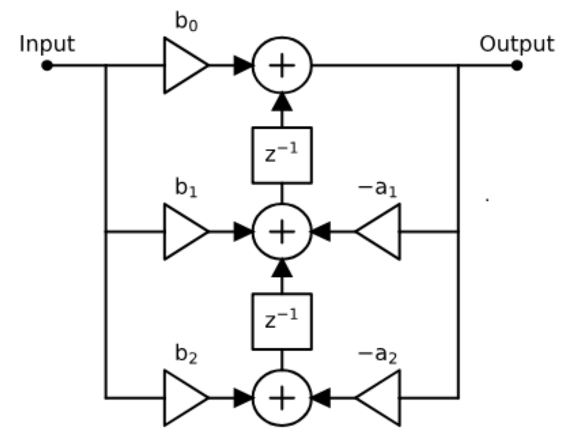

Figure 12: *Transposed direct form II filter structure.*

present two methods for adding nonlinear elements to the TDF-II structure that can create interesting sonic effects without affecting the filter's stability.

For the first method we propose adding nonlinear elements before the delay elements in the filter structure, as shown in fig. 13. When saturating nonlinearities are used for these elements, the filter exhibits "nonlinear resonance" similar to many analog filters. The filter frequency response at various operating points is shown in fig. 15.

For the second method we propose adding nonlinear elements to the feedback paths of the filter, as shown in fig. 14. Again, with saturating nonliearities, this structure causes the filter poles to "sweep" to different frequencies as the input level of the filter varies. The filter frequency response at various operating points is shown in fig. 16.

In order to maintain stability, we propose that the nonlinear elements must satisfy the constraint that $|f'_{NL}(x)| \leq 1$ (note that this implies that the derivative of the nonlinear function must exist everywhere in the range of x). A proof of this constraint using Lyapunov stability, as well as a more in-depth analysis of these nonlinear filter structures, including the potential use of these structures for analog modelling, is given in [6].

6. IMPLEMENTATION AND PRESENTATION

The work done in this study was designed to be informative and inspiring both to recording engineers and musicians, as well as programmers and aspiring DSP engineers looking to design audio effects. With this audience in mind, it was determined that the results of this work should be written and presented for a relatively non-technical reader, and published in a location where these readers would most easily find it. To that end, the results of this work have been published as a series of articles on the popular blog website Medium [1]. According to statistics on the site, the articles have been read approximately 300 times as of this writing. Additionally, the structures developed in this study have been implemented as a series of audio plugins using JUCE/C++. The plugins and their source code are freely available on GitHub [2].

7. CONCLUSION

In this paper, we have presented a series of complex nonlinear signal processing structures, with the intention of being used for audio effects and synthesis software. While this work has developed a number of useful and sonically rich structures, there is great potential for many more developements in this area of audio signal

[1]https://medium.com/@jatinchowdhury18
[2]https://github.com/jatinchowdhury18/ComplexNonlinearities

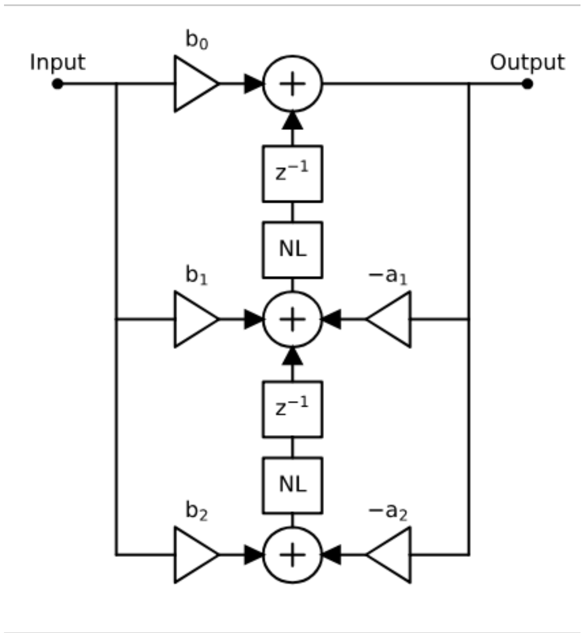

Figure 13: *Transposed direct form II with nonlinear resonance.*

processing. We look forward to seeing more audio effects being built using these methods, as well as to more nonlinear DSP methods being developed in the vein of this work.

8. ACKNOWLEDGMENTS

The author would like to thank Julius Smith, Kurt Werner, Viraga Perera, Dave Berners, and the GASP working group for providing inspiring discussions and indispensible feedback.

9. REFERENCES

[1] D.T. Yeh, *Digital Implementation of Musical Distortion Circuits by Analysis and Simulation*, Ph.D. thesis, Stanford Univeristy, 06 2009.

[2] Jatin Chowdhury, "Real-time physical modelling for analog tape machines," in *22nd International Conference on Digital Audio Effects*, Birmingham, UK, 2019, p. 3.

[3] Aphex Systems Ltd., *Aphex Aural Exciter Type B: Operating Guide*.

[4] Priyanka Shekar and Julius Smith, "Modeling the harmonic exciter," 10 2013.

[5] Dimitrios Giannoulis, Michael Massberg, and Joshua D. Reiss, "Digital dynamic range compressor design - a tutorial and analysis," *J. Audio Eng. Soc*, vol. 60, no. 6, pp. 399–408, 2012.

[6] Jatin Chowdhury, "Stable structures for nonlinear biquad filters," dec 2019.

[7] Francois Germain, *Non-oversampled physical modeling for virtual analog simulations*, Ph.D. thesis, Stanford University, 2019.

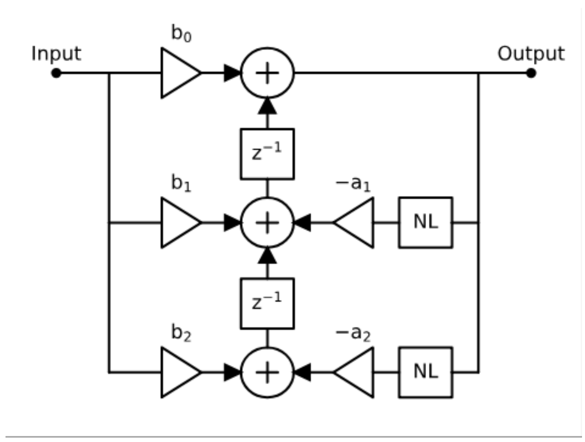

Figure 14: *Transposed direct form II with nonlinear feedback.*

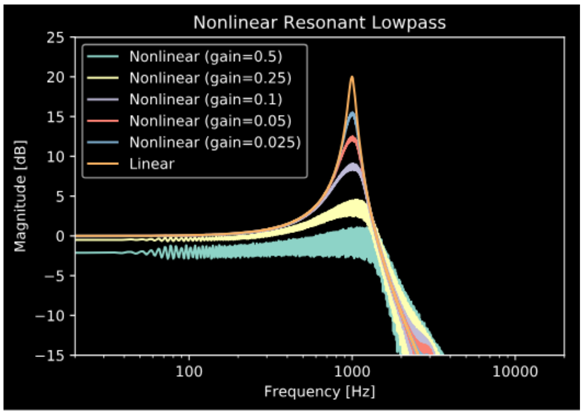

Figure 15: *Frequency response of nonlinear resonance filter at various operating points.*

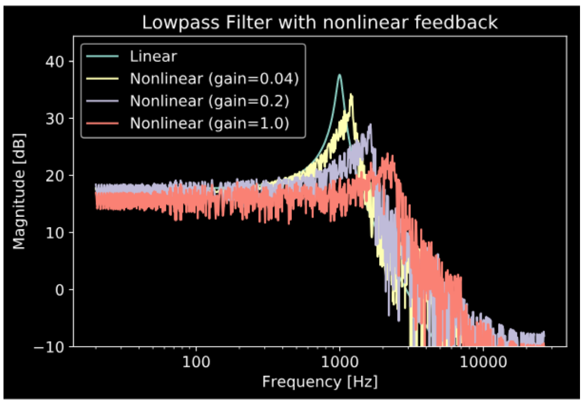

Figure 16: *Frequency response of nonlinear feedback filter at various operating points.*